



1 **Prediction of algal blooms via data-driven machine learning models:**

2 **An evaluation using data from a well monitored mesotrophic lake**

3 Shuqi Lin<sup>1\*</sup>, Donald C. Pierson<sup>1</sup>, Jorrit P. Mesman<sup>1,2</sup>

4 <sup>1</sup>Erken Laboratory and Limnology Department, Uppsala University, Uppsala, Sweden

5 <sup>2</sup>Département F.-A. Forel des sciences de l'environnement et de l'eau, Université de Genève, Genève,

6 Switzerland

7 *Correspondence to:* Shuqi Lin (Shuqi.lin@ebc.uu.se)

8 **Abstract.** With the increasing lake monitoring data, data-driven machine learning (ML) models might be able to  
9 capture the complex algal bloom dynamics that cannot be completely described in process-based (PB) models.  
10 We applied two ML models, Gradient Boost Regressor (GBR) and Long Short-Term Memory (LSTM) network,  
11 to predict algal blooms and seasonal changes in algal chlorophyll concentrations (*Chl*) in a mesotrophic lake.  
12 Three predictive workflows were tested, one based solely on available measurements, and the others applying a  
13 two-step approach, first estimating lake nutrients that have limited observations, and then predicting *Chl* using  
14 observed and pre-generated environmental factors. The third workflow was developed by using hydrodynamic  
15 data derived from a PB model as additional training features in the two-step ML approach. The performance of  
16 the ML models was superior to a PB model in predicting nutrients and *Chl*. The hybrid model further improved  
17 the prediction of the timing and magnitude of algal blooms. A data sparsity test based on shuffling the order of  
18 training and testing years showed the accuracy of ML models decreased with increasing sample interval, and  
19 model performance varied with training/testing year combinations.

20 **1 Introduction**

21 Harmful algal blooms, which are a serious threat to natural water systems, have been increasing throughout the  
22 world (Burford et al., 2020; Watson et al., 2016), primarily as a consequence of both climate change and increased  
23 nutrient loading from anthropogenic activities (Brookes and Carey, 2011; Paerl and Huisman, 2008). Moreover,  
24 as indicated by Carey et al. (2012) and Huisman et al. (2018), more intense and longer periods of thermal  
25 stratification could potentially specifically favour blooms of toxic cyanobacteria. To better manage and mitigate  
26 the effects of algal blooms, methods to forecast their timing and magnitude are needed. However, the factors  
27 regulating algal blooms are complex, variable and site-specific, often involving high-order interactions of  
28 environmental factors and biogeochemical processes (Reichwaldt and Ghadouani, 2012; Richardson et al., 2018).



29 Process Based (PB) models encode our understanding of biogeochemical processes into a framework of numerical  
30 formulations, but these are inevitable simplifications that lead to an incomplete description of complex  
31 biogeochemical interactions (Elliott, 2012).

32 With the proliferation of lake monitoring data (Marcé et al., 2016), data-driven machine learning (ML) approaches  
33 have been applied, as an alternative to PB models for bloom prediction (Rousso et al., 2020). Previously applied  
34 ML models, including Random Forest (Recknagel et al., 1998), Support Vector Machine (Jimeno-Sáez et al.,  
35 2020), and Artificial Neural Network (Xiao et al., 2017; Nelson et al., 2018; Wei et al., 2001), can improve  
36 predictions of the timing and seasonality of algal *Chl* pattern, apparently by accounting for complexity that is  
37 difficult to encode within the framework of a PB model.

38 In this study, we propose a two-step ML approach for predicting algal dynamics that: first estimates lake nutrient  
39 concentrations which often have limited observations and secondly predicts variations in algal *Chl* using these  
40 pre-generated nutrient concentrations combined with other observed environmental factors that are collected at  
41 higher frequency. We also test a simple hybrid model architecture that by adding hydrodynamic features derived  
42 from the PB model into the training features of the two-step ML approach, allowing us to include additional  
43 information describing physical lake processes expected to affect variations in algal growth and succession in the  
44 machine learning prediction.

45 We applied the above workflows to predict changing *Chl* concentration, as a proxy for the occurrence of algal  
46 blooms, via Gradient Boost Regressor (GBR) and Long Short-term Memory network (LSTM). Two shuffling  
47 year tests were conducted. One assessed the uncertainty of ML models in predicting *Chl* during the same two-  
48 year period and the other evaluated the sensitivity of ML accuracy to various training/testing year combinations  
49 and lake nutrient sampling intervals. Model performance and potential applications in algal bloom forecasting are  
50 discussed.

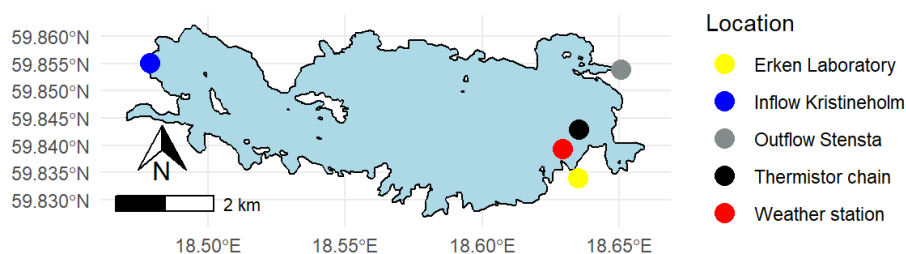
## 51 **2 Methods**

### 52 **2.1 Study site**

53 The study site, Lake Erken, is a mesotrophic lake located in east-central Sweden, that has a surface area of 24  
54 km<sup>2</sup>, a maximum depth of 21 m and an average retention time of 7 years. The lake is dimictic with seasonal  
55 stratification commonly beginning in May-June and ending in August-September. The onset of ice cover usually  
56 begins in December-February and the loss of ice occurs in Mar-April (Persson and Jones, 2008). Located near the  
57 Baltic coast, Lake Erken is wind exposed, and susceptible to periodic wind-induced turbulent mixing.



58 Changes in algal *Chl* in Lake Erken have a typical seasonal pattern, with spring and summer peaks in concentration  
59 (Pettersson et al., 2003). Spring blooms are dominated by dinoflagellates and diatoms (Pettersson, 1985), and  
60 initiated by overwinter species from the last autumn (Yang et al., 2016). Cyanobacteria dominate summer peaks  
61 in *Chl*, given that they can optimize their vertical position in regarding to nutrients and light (Paerl, 1988; Pierson  
62 et al., 1992).



63  
64 **Figure 1.** Map of Lake Erken. The locations of the monitoring systems are shown.

## 65 2.2 Data

66 Lake Erken has a long running automated monitoring program that provides hourly meteorological data, water  
67 temperature profiles between 0.5 and 15 m at 0.5 m intervals and the flow from the inflow and outflow (Fig.1). A  
68 manual sampling program collects samples during ice-free time at 5-7 days intervals for all major nutrient  
69 concentrations (e.g., NO<sub>x</sub>, NH<sub>4</sub>, PO<sub>4</sub>, Total P, Si, etc.), dissolved oxygen (O<sub>2</sub>), and *Chl* concentration. The timing  
70 of the onset and loss of ice cover are also monitored yearly by the lab. More detailed information on the sampling  
71 program is in Supporting Information (See Text S1) and Moras et al. (2019).

## 72 2.3 Modelling Methods

### 73 2.3.1 Process-based (PB) lake model

74 In this study, a PB hydrodynamic lake model, GOTM (General Ocean Turbulence Model) (Burchard et al., 1999),  
75 was used to generate water temperature profiles, and other hydrodynamic metrics. GOTM also served as the  
76 foundation of water quality simulations made with the SELMAPROTBAS model (Mesman et al., 2022) that is  
77 coupled to GOTM through the Framework for Aquatic Biogeochemical Models FABM (Bruggeman and Bolding,  
78 2014).

### 79 2.3.2 Data-driven machine learning (ML) models

80 Two ML models were evaluated in this study. Gradient Boosting Regressor (GBR) which iteratively generates an  
81 ensemble of estimator trees with each tree improving upon the performance of the previous (Friedman, 2001), and



82 Long short-term memory (LSTM) networks which is built for sequential and timeseries modelling (Hochreiter  
83 and Schmidhuber (1997), See Fig. S2, SI). The hyperparameter settings in both ML models can be found in  
84 Supporting Information (See Text S2). Both ML models are built on Python using the Scikit-Learn (<https://scikit-learn.org/stable/>, last access: September, 2021) and TensorFlow (<https://www.tensorflow.org/>, last access:  
85 September, 2021) libraries.

#### 87 **2.4 Design of predictive workflows and shuffling year data sparsity tests**

88 In this study, we tested three workflows using a dataset split for training (years 2004-2016) and testing (years  
89 2017-2020). In all three workflows, a 5-fold cross-validation using the training dataset was used to optimize the  
90 hyperparameters in the ML models. Workflow 1 directly predicts *Chl* concentration based on available  
91 environmental observations (See SI, Table S1). The training and testing datasets were limited by the frequency of  
92 lake nutrient observations which resulted in 5-7 days gap between data points. The time step of LSTM was set to  
93 1, that is, the environmental factors on the target date and previous observation date, which may be 5-7 days ago,  
94 were used to train the model and make predictions.

95 In workflow 2 and 3, a two-step approach was applied (Table S1). Daily measurements of physical factors were  
96 used to pre-generate daily variations in lake nutrients via separate ML models, and the ML models were trained  
97 at a daily time step using the measured environmental factors and pre-generated nutrient concentrations. The time  
98 step of LSTM was then set to 7 days.

99 In workflow 3, three hydrodynamic features, i.e., mixing layer depth ( $z_e$ ), Wedderburn number ( $W_n$ ), and the  
100 seasonal thermocline depth (*thermD*), derived from the GOTM model were regarded as daily training features in  
101 the two-step ML approach. The definitions and calculations of these features are explained in SI (2.5 Feature  
102 selection and processing for ML models, Text S3)

103 Following the two-step approach and using workflow 3, we set up two tests. (1) To assess the uncertainty induced  
104 by variations in the data used to train the ML models, we shuffled the training years, randomly taking 13 years  
105 out of 2004-2018 dataset 30 times, and tested the model predictions of *Chl* during 2019-2020. And, (2) to test if  
106 the workflow could be used for other water systems which may have less frequent lake nutrient monitoring data,  
107 we conducted a data sparsity test that evaluated the sensitivity of models to the lake nutrient and *Chl* sampling  
108 interval. For this test the lake nutrient and *Chl* concentration observations in training dataset was down-sampled  
109 to a 7-day, 14-day, 21-day, 28-day, and 35-day sampling interval. Then for each sampling interval using the 2004-  
110 2020 dataset, *Chl* was predicted for different consecutive 4-year periods when the ML models were trained by the



111 remaining 13 years of data. Data shuffling was conducted 13 times so that every 4-year period in our dataset was  
112 tested.

### 113 **2.5 Feature selection and processing for ML models**

114 The feature selection process is based on some a priori knowledge of the underlying phenomena related to algal  
115 blooms. All workflows made use of the daily automated monitoring data. In addition, the temperature difference  
116 ( $\Delta T$ ) between surface water (averaged over the upper 3 m) and bottom water (15 m) was also used to represent  
117 the thermal structure of the lake., and the duration of ice cover in the previous winter, and the number of days  
118 from ice-off date were used.

119 In workflow 2 and 3 nutrients are predicted sequentially, with each pre-generated nutrient predictions included in  
120 the training data of the next nutrient prediction (Table S1). Workflow 3 added  $z_e$ , computed using the GOTM  
121 simulated vertical eddy diffusivity ( $K_z$ ) profiles,  $thermD$ , estimated using Lake Analyzer (Read et al., 2011) based  
122 on GOTM simulated temperature profile, and  $W_n$ , a dimensionless parameter measuring the balance between wind  
123 stress and the pressure gradient resulting from the slope of the interface (See Text S3, SI), as additional daily  
124 training features.

### 125 **2.6 Evaluating metrics**

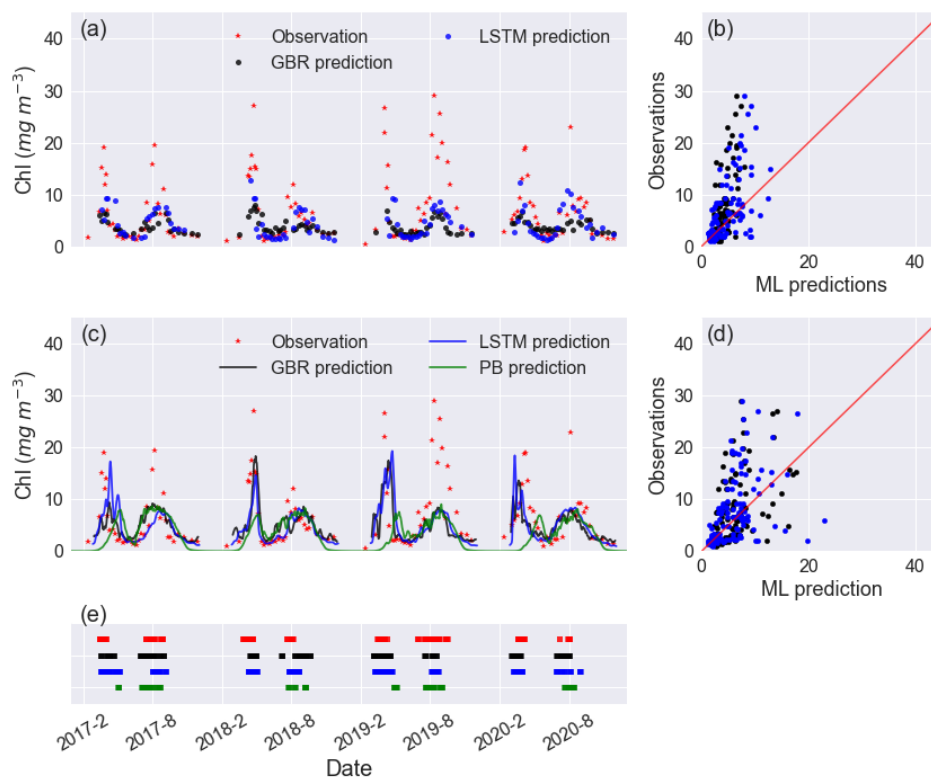
126 Model performance was evaluated by comparing the simulated and measured *Chl* concentrations, and by  
127 calculating the mean absolute error (*MAE*), root means square error (*RMSE*), and correlation coefficient ( $R^2$ ). To  
128 evaluate the accuracy of the model in detecting the onset of an algal bloom, we calculated a confusion matrix in  
129 workflows 2 and 3, where the observations were linearly interpolated to daily values, and predicted daily *Chl*  
130 concentration were smoothed with a 7-day rolling mean. Using these data, the onset of a bloom was categorized  
131 as occurring when the daily change of *Chl* ( $\Delta Chl$ ) exceed a threshold,  $0.35 \text{ mg m}^{-3} \text{ day}^{-1}$ . This works well in Lake  
132 Erken where *Chl* concentrations are frequently monitored (near weekly), and the linear interpolation can be  
133 expected to be reasonably representative of the *Chl* concentrations between measured samples. Considering the  
134 randomization in the ML models, we also add a 3-day window on the bloom onset prediction, that is, we  
135 considered the prediction of a bloom valid if the measured data suggested a bloom the day before or after the  
136 simulated onset. We used the True Positive Rate (TPR), False Positive Rate (FPR), and modified accuracy Kappa  
137 (Mchugh, 2012) to identify the potential of ML models to correctly capture the algal bloom onset (See Table S2,  
138 SI). A model with 100% TPR, 0% FPR, and 100% Kappa would constitute a perfect fit.



139 **3 Results**

140 **3.1 Workflow 1: Direct prediction based on observations**

141 In workflow 1, both GBR and LSTM clearly reproduced spring and summer blooms (Fig. 2a) but underestimated  
142 the intensity of blooms (Fig. 2a, b). Neither ML model captured the extraordinarily high *Chl* (~15-30 mg m<sup>-3</sup>) in  
143 the summer of 2019. The cross-validation on training dataset (See Table S3, SI) shows what appears to be  
144 overfitting issue in both models, with somewhat higher *RMSE* and *MAE* in the testing dataset than the mean values  
145 in the training dataset. The achieved accuracy of models is attributed to the daily availability of physical inputs,  
146 and the fact that in Lake Erken water samples are collected frequently at 5-7 days intervals. Workflow 1 may be  
147 most valuable in reconstructing previous variations in algal *Chl*, filling the gaps between measured *Chl*  
148 observations and feature importance ranking (See Fig. S4, SI). But when using this workflow future forecasts will  
149 be limited by the absence of future nutrient data.



150

151 **Figure 2.** Timeseries of observed and predicted *Chl* from GBR and LSTM models in (a) workflow 1 and (c)  
152 workflow 3, and the corresponding scatter plots of observations vs ML predictions of *Chl* in workflow 1 and  
153 workflow 3 are shown in panels (b) and (d), with the black and blue dots/lines representing the predictions from



154 GBR and LSTM, respectively. Panel (e) shows the observed and predicted algal bloom onsets in 2017-2020 using  
155 the same color coding as the previous panels. Results from the PB model simulation in Mesman et al. (2022) are  
156 also shown in (c) and (e).

### 157 **3.2 Workflow 2: Two-step ML models based on pre-generated daily nutrients and observed physical** 158 **factors**

159 As in workflow 1, both ML models in workflow 2 suffered from overfitting with higher *MAE*, *RMSE*, and lower  
160 *R*<sup>2</sup> in testing datasets than training datasets (See SI, Table S3).

161 Overall, both GBR and LSTM showed slightly higher *MAE* (4.22 mg m<sup>-3</sup> vs. 3.87 mg m<sup>-3</sup>) and *RMSE* (6.27 mg  
162 m<sup>-3</sup> vs. 6.00 mg m<sup>-3</sup>) when compared to workflow 1 (Table 1). But they also showed improved performance in  
163 terms of capturing the peak values of *Chl* during spring blooms (Fig. 2, Fig. S5, SI). Both workflows outperformed  
164 the SELMAPROTBAS PB model in simulating concentrations of lake nutrients (See Fig. S6, SI). The ML models  
165 were more accurate in predicting the low values of NO<sub>x</sub> and peak values of PO<sub>4</sub> and Total P. However, both ML  
166 models and the PB model failed in predicting the extremely high values of measured lake nutrients, such as the  
167 autumn peak of NH<sub>4</sub> in 2017 (Fig. S6e) and the spring peak of O<sub>2</sub> in 2018 (Fig. S6c), Thus, higher workflow 2  
168 *MAE* and *RMSE* (Table 1) are presumably due to the inaccuracies in the pre-generated nutrient training data, but  
169 the improved daily predictions that better capture the bloom events, overshadow these flaws.

170 **Table 1.** Comparisons of model performance during the testing period based on *RMSE*, *MAE*, and *R*<sup>2</sup>. The unit  
171 of *Chl* is mg m<sup>-3</sup>.

Model	PB	ML-workflow 1		ML-workflow 2		ML-workflow 3	
		GBR	LSTM	GBR	LSTM	GBR	LSTM
<i>RMSE</i>	7.18	5.77	<b>5.64</b>	6.27	6.00	5.94	5.81
<i>MAE</i>	4.77	<b>3.55</b>	3.58	4.22	3.87	3.99	3.71
<i>R</i> <sup>2</sup>	-0.25	0.13	<b>0.20</b>	0.05	0.13	0.14	0.18

172

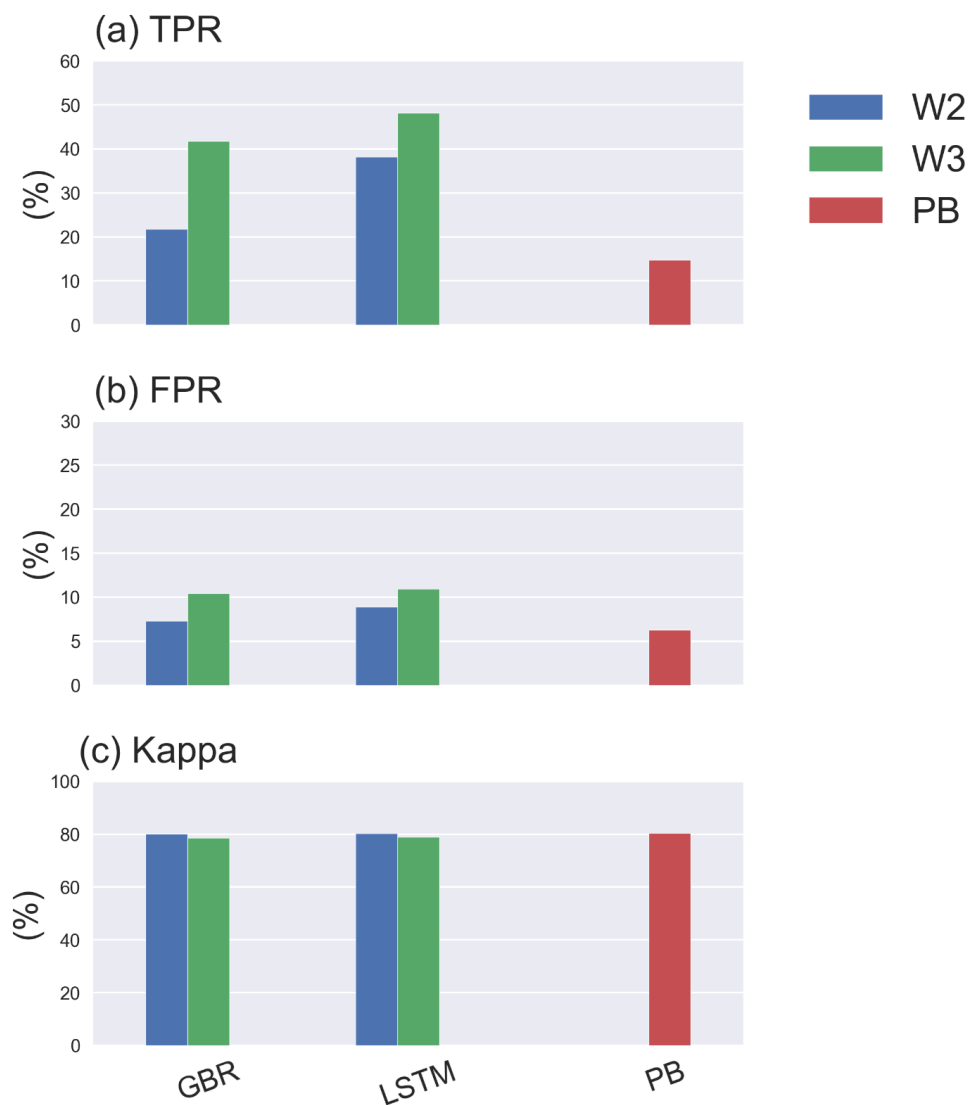
### 173 **3.3 Workflow 3: based on workflow 2, and including hydrodynamic training features derived from the** 174 **GOTM model.**

175 Including hydrodynamic training information in workflow 3 did not significantly improve in lake nutrient  
176 predictions compared to workflow 2 (See Fig. S6), and when using workflow 3 both ML models showed  
177 comparable performance in *Chl* predictions compared to workflow 1. However, the predictions of the spring  
178 bloom in all years improved compared to workflows 1 and 2, in terms of the magnitude and timing of spring  
179 bloom (Fig. 2e). This was the case in 2019-2020 (Fig. 2a) which was an abnormally warm winter with only 5 days



180 ice cover, and had an unusually early spring algal bloom. Both workflow 2 and 3 did not capture the extremely  
181 intensive bloom (with peak values closed to  $30 \text{ mg m}^{-3}$ ) in summer of 2019, and neither did the PB model.  
182 Furthermore, adding hydrodynamic features derived from PB model improved predictions of the onset of algal  
183 blooms (Fig. 2e and 4), with the overall TPR increasing by 15 % and 5 %, FPR increasing around 5 % and 3 % in  
184 GBR and LSTM models, respectively. Compared with the PB model which showed lower TPR (15%) and FPR  
185 (6%), ML models are more likely to predict algal bloom at the correct time. However, the concomitant higher  
186 FPRs indicating an incorrect warning of algal bloom is also more likely to occur in the ML models, since the PB  
187 model is more like to miss the bloom entirely. The Kappa values of both ML models and the PB model are close  
188 to 80%, showing that all models simulated the entire period (blooms and the periods between blooms) to a  
189 moderate-strong level (Mchugh, 2012).





190

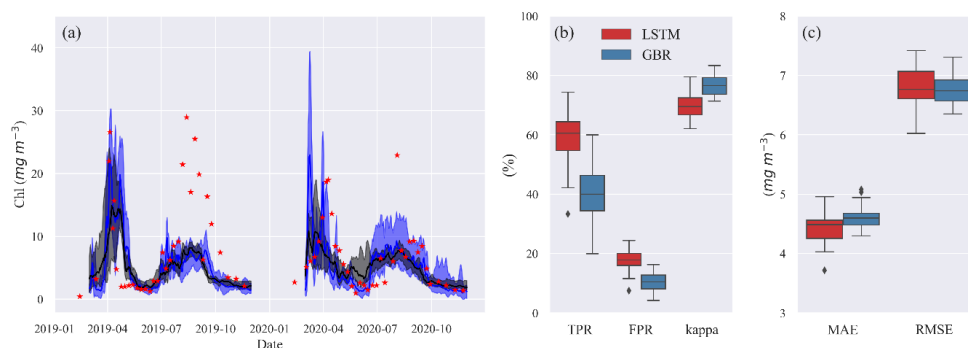
191 **Figure 3.** TPR, FPR, Kappa of GBR and LSTM models in workflow 2, 3 and the PB model.

### 192 3.4 Effects of shuffling training years on 2019-2020 predictions

193 The results presented so far are based on a typical strategy of training ML models for a historical period in this  
194 case 2004-2016 and then accessing model performance in a second period between 2017-2020. The accuracy of  
195 the model predictions will to some extent be related to the range and variability in the training data. To evaluate  
196 the importance of this we randomly removed two years from a 2004-2018 training dataset, and made 30 different  
197 predictions of *Chl* during 2019-2020 when the models had difficulties predicting spring and summer blooms (Fig  
198 5). When trained with the various shuffled combinations, both ML models were capable of reproducing the



199 seasonal variations in algal *Chl* with a 4.5 % and 5.8 % coefficient of variation (CV) in *MAE*, and a 24.0 % and  
200 16.4 % CV in TPR of GBR and LSTM, respectively (See Table S4, SI). This provides an indication of the  
201 uncertainty that may arise as a consequence of differences in the training datasets used for in our workflows. And,  
202 it also shows that even a relatively long training period of 13 years can not totally capture the system behaviour  
203 in such a way as to lead to nearly similar bloom predictions.  
204 Although none of the model runs captured the intensive summer bloom in 2019, the spring bloom in both years  
205 was well represented, especially by LSTM, in terms of timing and magnitude.



206  
207 **Figure 4.** (a) Timeseries of observed (red stars) and predicted *Chl* from GBR (black) and LSTM (blue) models in  
208 shuffling training year test. The shades represent the range between minimum and maximum prediction, and the  
209 solid lines represent the median prediction.

210  
211 Despite comparable *RMSE* and *MAE* in LSTM and GBR (Fig. 4c), both higher TPRs (with median of 60%) and  
212 FRPs (with median of 18%) in LSTM indicate that the LSTM was more aggressive in making algal bloom  
213 predictions. The GBR model's apparent advantage in FPRs (with median 10%) is largely the result of it making  
214 a lower number of bloom predictions since the low concentrations between spring and summer blooms in 2020  
215 was not well represented (Fig. 4b).

### 216 3.5 Shuffling years data sparsity test

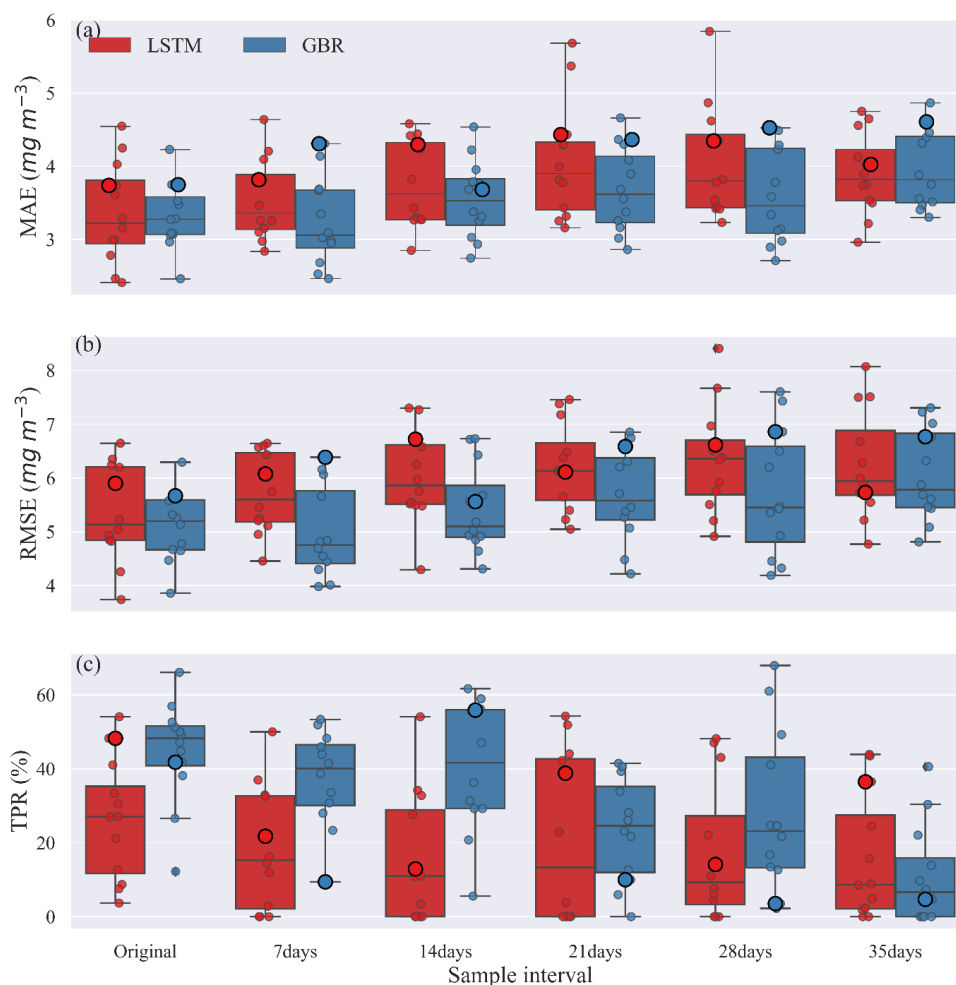
217 To examine the possible use of workflow 3 when data are less frequently available, lake nutrient and *Chl* data  
218 were down-sampled so that the effects of sampling frequency on model predictions could be evaluated. Each  
219 down-sampled dataset was also rearranged into 13 different 13-year training periods and 4-year testing periods.  
220 The variability in predictions provided a measure of model performance and uncertainty. Fig. 5 shows the  
221 uncertainty in model predictions as a consequence of the chosen sampling intervals.

222 The *MAEs* and *RMSEs* of both GBR and LSTM models tended to increase with the longer sample intervals. The  
223 median *MAE* was always slightly higher for the LSTM model except when trained with original dataset (Fig. 5a).



224 While our initial evaluation of TPR using 2017-2020 as the testing period and 2004-2016 as the training period  
225 suggested the LSTM model was more accurate in turns of detection of algal bloom onsets (Fig. 3), Fig. 5c showed  
226 the median TPR of GBR model over was over 50%, higher than LSTM model. This can be explained by the fact  
227 that the 2017-2020 period as in Fig. 3 and shown as large points in Fig. 5 was unusually difficult for GBR to  
228 simulate. Consequently, even though the GBR model usually performs better in Fig. 5c the testing period chosen  
229 for use in Fig. 3, showed the opposite result. This illustrates the importance of the sequence of training and testing  
230 years for evaluating model performance.

231 For the first three sampling intervals the GBR model clearly had better TPR values than the LSTM model. The  
232 median TPRs of GBR model started to drop below 30% once the sample interval reached 21 days. For LSTM,  
233 median TPRs remained lower than 30%, for all sampling intervals but also showed a much wider range of  
234 variability (Table S5) dependent on the training and tested datasets used. In general, both models performed best  
235 at the original and 7-day sampling interval, but then showed slightly worse performance that was consistent up to  
236 a sample interval of 21 days. In terms of the errors evaluated over the entire 4-year testing period (Fig. 5a, b) the  
237 GBR model had lower errors and therefore, better, predicted the seasonal variations of *Chl* concentration. The  
238 timeseries comparison of observed and predicted *Chl* from this shuffling year data sparsity test can be found in SI  
239 (Fig. S7-9).



240

241 **Figure 5.** Comparisons of (a) *MAE*, (b) *RMSE*, and (c) *TPR* between GBR and LSTM under various sample  
242 intervals. Circles along the box show the result from every training and testing years combination and the bigger  
243 circles represent 2004-2016 training and 2017-2020 testing years combination as was used in Fig. 2.

## 244 4 Discussion

### 245 4.1 Performance of ML models

246 In three workflows, the ML models successfully reproduced the *Chl* seasonal patterns, capturing the spring and  
247 summer bloom events, with lower averaged *RMSEs* and *MAEs* than PB model simulations that was previously  
248 calibrated for use in Lake Erken. Workflow 1 which predicted *Chl* based on all available environmental factors  
249 including lake nutrient observations showed that both ML models can reproduce the seasonal dynamics of algal  
250 *Chl* with promising accuracy (*MAE* = 3.55 and 3.58 mg m<sup>-3</sup>, *RMSE* = 5.77 and 5.64 mg m<sup>-3</sup> and *R*<sup>2</sup> = 0.13 and



251 0.20) via the direct input of available environmental observations. These ML models can be applied to reconstruct  
252 past patterns of algal *Chl*, fill the gaps between measured *Chl* observations, and interpret the mechanisms that  
253 drive phytoplankton dynamics. Workflows 2 and 3 adopted a two-step approach, first using separate ML models  
254 to estimating daily changes in lake nutrient concentration, and in Workflow 3 also including PB model derived  
255 physical factors as training features of the algal ML model. These two workflows allowed daily predictions of  
256 changes in algal *Chl* concentration using both observations and pre-generated lake nutrient concentrations at a  
257 consistent daily time step, and achieved comparable accuracy in *Chl* prediction to workflow 1, demonstrating the  
258 potential for making daily forecasts without measured nutrient observations.

259 However, there was overfitting issues in all three workflows, in both GBR and LSTM models, indicated by higher  
260 *MAE* and *RMSE* in the testing dataset compared to the training dataset especially for GBR (Table S3).

261 The one clear failure of both the ML and PB based model predictions was during July-August 2019, *Chl*  
262 concentrations in integrated samples collected between the surface and 6-12 m exceeded 20 mg m<sup>-3</sup> over a 5-week  
263 period. Neither the PB model nor ML models captured this unusually persistent bloom (Fig. 2, Fig. S3, SI). At  
264 this time the phytoplankton were dominated by the cyanobacteria *Gloeotrichia* and *Anabaena*, that form a resting  
265 akinete life stage at the end of their yearly bloom, which can initiate the following year's bloom as they are  
266 transformed to vegetative cells that migrate from the sediment to the upper water column. We hypothesize that  
267 the large summer bloom in 2019 was the result of unusually large recruitment of akinetes in this year. (Karlsson-  
268 Elfgrén et al., 2005; Karlsson-Elfgrén et al., 2004). The life cycle of cyanobacteria is not a process included in the  
269 PB model (but see Hense and Beckmann (2006) and Jöhnk et al. (2011)), so increased recruitment of akinetes  
270 could explain the underestimation of the 2019 summer bloom. Even the LSTM algorithms could not account for  
271 previous condition so far back in time as to affect the formation and deposition of cyanobacteria akinetes.

272 Warm winters can initiate a chain of events, i.e., shortening the ice cover duration, extending spring circulation,  
273 affected nutrients availability, and an earlier spring bloom (Adrian et al., 2006; Yang et al., 2016). According to  
274 the ice record in Lake Erken (See Fig. S1, SI), in 2020, the lake was covered by very thin ice for only 5 days,  
275 which is the shortest duration since observations were first recorded in 1954. The spring bloom in 2020 did occur  
276 earlier than other years (See Fig. S3, SI), and both ML models which considered the timing of lake ice show fairly  
277 good performance in predicting the timing and magnitude of this abnormally early spring bloom (Fig. 2, 5)

#### 278 4.1.1 Performance of Hybrid PB ML models

279 One dimensional PB hydrodynamic models can accurately simulate both water temperature profiles, and other  
280 hydrodynamic features in Lake Erken using the same forcing data that are commonly input to ML models. The



281 hybrid model structure tested here provides a richer set of input data leading to more accurate ML predictions of  
282 algal *Chl* at little additional computational cost or data requirements. Using data from the hydrothermal PB model  
283 allowed the seasonal deepening of the thermocline, variations in the surface mixing layer depth, and upwelling  
284 events, represented by  $W_n$ , to be encoded into the ML algorithms. These factors can affect the underwater light  
285 climate, the internal loading of phosphorus and the transport of resting cyanobacteria colonies from the  
286 hypolimnion into the epilimnion favouring summer blooms of cyanobacteria (Pierson et al., 1992; Pettersson,  
287 1998). The inclusion of these factors did increase the accuracy of the ML models, especially in the case of unusual  
288 environmental conditions (e.g. spring of 2020, Fig. 2, 5) that did not frequently occur in the remaining  
289 meteorological, hydrological and biogeochemical training data.

#### 290 4.1.2 Prediction of bloom timing

291 For the purposes of water management, it may be most important to first predict the potential occurrence of a  
292 bloom, and then once underway improve predictions of its magnitude. The best model performance in predicting  
293 the timing of algal blooms, was obtained after adding hydrodynamic features derived from a PB model in  
294 workflow 3, with TPR above 45% in detecting the onset of algal bloom during 2017-2020 and a modified accuracy  
295 (Kappa) around 80 % indicated a moderate – strong level of prediction.

296 Based on our shuffling year tests of bloom timing, the GBR model showed relatively higher median TPRs than  
297 LSTM model for sample intervals less than one month. However, in some training and testing year combinations,  
298 TPRs are close to 0 % (Fig. 5), and CVs of the TPRs are highly variable, even at the original sample interval,  
299 being over 30% for GBR and over 60% for LSTM, indicating that the correct detection of algal blooms in both  
300 models are highly dependent on the years used to train the models. Thus, while the ML models can be better than  
301 the PB models at predicting the onset of algal blooms, they still may not be good enough for operational  
302 forecasting. The resulting variability provided a more accurate estimate of the model performance at each down-  
303 sampled data interval and showed that increasing sample interval led to reduced performance for both ML models,  
304 in terms of *MAE*, *RMSE*, and the CV of TPR. These tests also highlighted that the performance of both ML models,  
305 especially LSTM, varied with the sampled history of events in the training period for evaluating a specific pattern  
306 of change in the testing period. We suggest that testing strategies similar to the shuffle methods used in this study  
307 are needed to accurately evaluate the expected accuracy of ML models when applied to any given site. The  
308 estimated uncertainty in shuffling training year tests (Fig. 4) and shuffling training/testing year tests (Fig. 5) can  
309 be used to better represent the uncertainty of ML derived forecasts.



#### 310 **4.2 Future applications in short-term forecasts and water management**

311 To reach the goal of incorporating ML models into operational forecasts either for short-term management support  
312 or longer-term evaluation and planning, two steps must occur. First the ML model must be developed, trained and  
313 evaluated on the water body of interest due to the unique physical characteristics and water quality dynamics in  
314 different systems. Secondly, future forcing data for the model must be obtained and integrated into a workflow  
315 that makes the future predications. In regards to the second point, a lack of frequent water monitoring (Stanley et  
316 al., 2019) is a major deterrence to applying ML models to many lakes. The data sparsity test (Fig. 5) showed that,  
317 at least for Lake Erken, the ML models can still detect the seasonal algal dynamics even for sample intervals  
318 approaching one month (Fig. S7-9). If this result holds for other lakes, the use of the two-step ML workflow could  
319 offer a method of forecasting seasonal variations in algal *Chl* even in lakes with relatively infrequent nutrient  
320 monitoring but higher frequency meteorological and hydrological data.

321 The hybrid PB/ML models have the potential to provide reasonably accurate and timely short-term algal bloom  
322 forecasts, working as part of an early-warning systems for the water resource management (Baracchini et al.,  
323 2020), and clearly have the ability to predict border seasonal variations in algal *Chl* concentration. However, since  
324 a large amount of water temperature and water quality samples are required for ML training, and since our results  
325 apply to only one well-studied lake, obtaining more datasets to test and evaluate the workflows developed here  
326 are needed. Monitoring networks (e.g., Global Lake Ecological Observatory Network [GLEON,  
327 <https://gleon.org/>]), could provide the data to allow more extensive testing and application of hybrid PB/ML  
328 models, and we are presently working in the GLEON network to test the methods developed in this paper on many  
329 other lakes.

#### 330 **5 Code availability**

331 Model version 1.0 has been archived in Zenodo under [DOI: 10.5281/zenodo.6534790](https://doi.org/10.5281/zenodo.6534790), and is available at  
332 [https://github.com/Shuqi-Lin/Erken\\_Algal\\_Bloom\\_Machine\\_Learning\\_Model.git](https://github.com/Shuqi-Lin/Erken_Algal_Bloom_Machine_Learning_Model.git).

#### 333 **6 Data availability**

334 Lake Erken data are provided by Erken Laboratory, Uppsala University (<https://www.ieg.uu.se/erken-laboratory/lake-monitoring-programme/>, last access: May 2022). The dataset has been made possibly by the  
335 Swedish Infrastructure for Ecosystem Science (SITES), in this cast at Lake Erken.  
336



337 **7 Supplement**

338 **8 Author contribution**

339 The concept of ML model workflow was designed by SL and DP. SL developed the ML model code and  
340 performed the simulations. JM conducted the PB model simulations. SL wrote the manuscript with contributions  
341 from DP and JM.

342 **9 Competing interests**

343 The contact author has declared that neither they nor their co-authors have any competing interests.

344 **10 Acknowledgement**

345 S.L. and this study are funded by the EU and FORMAS project 2018-02771, in the frame of the collaborative  
346 international Consortium BLOOWATER (<https://www.bloowater.eu/>) financed under the ERA-NET  
347 WaterWorks2017 Cofounded Call. This ERA-NET is an integral part of the 2018 Joint Activities developed by  
348 the Water Challenges for a Changing World Joint Program Initiative (Water JPI). J.P.M. was funded by the  
349 European Union's Horizon 2020 Research and Innovation Programme under grant agreements no. 722518  
350 (MANTEL ITN) and 101017861 (SMARTLAGOON). SITES receives funding through the Swedish Research  
351 Council under the grant no. 2017-00635.

352 **References**

- 353 Adrian, R., Wilhelm, S., and Gerten, D.: Life-history traits of lake plankton species may govern their phenological response  
354 to climate warming, *Global Change Biology*, 12, 652-661, 10.1111/j.1365-2486.2006.01125.x, 2006.
- 355 Baracchini, T., Wüest, A., and Bouffard, D.: Meteolakes: An operational online three-dimensional forecasting platform for  
356 lake hydrodynamics, *Water Research*, 172, 115529, 10.1016/j.watres.2020.115529, 2020.
- 357 Brookes, J. D. and Carey, C. C.: Resilience to Blooms, *Science*, 334, 46-47, doi:10.1126/science.1207349, 2011.
- 358 Bruggeman, J. and Bolding, K.: A general framework for aquatic biogeochemical models, *Environmental Modelling &*  
359 *Software*, 61, 249-265, <https://doi.org/10.1016/j.envsoft.2014.04.002>, 2014.
- 360 Burchard, H., Bolding, K., and Villarreal, M. R.: GOTM, a General Ocean Turbulence Model: Theory, Implementation and  
361 Test Cases, European Commission. Joint Research Centre, Space Applications Institute, 103,  
362 [https://books.google.be/books/about/GOTM\\_a\\_General\\_Ocean\\_Turbulence\\_Model.html?id=zsJUHAACA AJ&redir\\_esc=](https://books.google.be/books/about/GOTM_a_General_Ocean_Turbulence_Model.html?id=zsJUHAACA AJ&redir_esc=y)  
363 [y](https://books.google.be/books/about/GOTM_a_General_Ocean_Turbulence_Model.html?id=zsJUHAACA AJ&redir_esc=y), 1999.
- 364 Burford, M. A., Carey, C. C., Hamilton, D. P., Huisman, J., Paerl, H. W., Wood, S. A., and Wulff, A.: Perspective:  
365 Advancing the research agenda for improving understanding of cyanobacteria in a future of global change, *Harmful Algae*,  
366 91, 101601, <https://doi.org/10.1016/j.hal.2019.04.004>, 2020.
- 367 Carey, C. C., Ibelings, B. W., Hoffmann, E. P., Hamilton, D. P., and Brookes, J. D.: Eco-physiological adaptations that  
368 favour freshwater cyanobacteria in a changing climate, *Water Research*, 46, 1394-1407, 10.1016/j.watres.2011.12.016, 2012.
- 369 Elliott, J. A.: Is the future blue-green? A review of the current model predictions of how climate change could affect pelagic  
370 freshwater cyanobacteria, *Water Research*, 46, 1364-1371, 10.1016/j.watres.2011.12.018, 2012.
- 371 Friedman, J. H.: Greedy Function Approximation: A Gradient Boosting Machine, *The Annals of Statistics*, 29, 1189-1232,  
372 2001.
- 373 Hense, I. and Beckmann, A.: Towards a model of cyanobacteria life cycle—effects of growing and resting stages on bloom  
374 formation of N<sub>2</sub>-fixing species, *Ecological Modelling*, 195, 205-218, <https://doi.org/10.1016/j.ecolmodel.2005.11.018>, 2006.
- 375 Hochreiter, S. and Schmidhuber, J.: Long Short-Term Memory, *Neural Computation*, 9, 1735-1780,  
376 10.1162/neco.1997.9.8.1735, 1997.





- 377 Huisman, J., Codd, G. A., Paerl, H. W., Ibelings, B. W., Verspagen, J. M. H., and Visser, P. M.: Cyanobacterial blooms,  
378 Nature Reviews Microbiology, 16, 471-483, 10.1038/s41579-018-0040-1, 2018.
- 379 Jimeno-Sáez, P., Senent-Aparicio, J., Cecilia, J. M., and Pérez-Sánchez, J.: Using Machine-Learning Algorithms for  
380 Eutrophication Modeling: Case Study of Mar Menor Lagoon (Spain), International Journal of Environmental Research and  
381 Public Health, 17, 1189, 2020.
- 382 Jöhnk, K. D., Brüggemann, R., Rucker, J., Luther, B., Simon, U., Nixdorf, B., and Wiedner, C.: Modelling life cycle and  
383 population dynamics of Nostocales (cyanobacteria), Environmental Modelling & Software, 26, 669-677,  
384 <https://doi.org/10.1016/j.envsoft.2010.11.001>, 2011.
- 385 Karlsson-Elfgren, I., Hyenstrand, P., and Riydin, E.: Pelagic growth and colony division of *Gloeotrichia echinulata* in Lake  
386 Erken, Journal of Plankton Research, 27, 145-151, DOI 10.1093/plankt/fbh165, 2005.
- 387 Karlsson-Elfgren, I., Rengefors, K., and Gustafsson, S.: Factors regulating recruitment from the sediment to the water  
388 column in the bloom-forming cyanobacterium *Gloeotrichia echinulata*, Freshwater Biology, 49, 265-273, DOI  
389 10.1111/j.1365-2427.2004.01182.x, 2004.
- 390 Marcé, R., George, G., Buscarinu, P., Deidda, M., Dunalska, J., de Eyto, E., Flaim, G., Grossart, H.-P., Istvanovics, V.,  
391 Lenhardt, M., Moreno-Ostos, E., Obrador, B., Ostrovsky, I., Pierson, D. C., Potužák, J., Poikane, S., Rinke, K., Rodríguez-  
392 Mozaz, S., Staehr, P. A., Šumberová, K., Waajen, G., Weyhenmeyer, G. A., Weathers, K. C., Zion, M., Ibelings, B. W., and  
393 Jennings, E.: Automatic High Frequency Monitoring for Improved Lake and Reservoir Management, Environmental Science  
394 & Technology, 50, 10780-10794, 10.1021/acs.est.6b01604, 2016.
- 395 McHugh, M. L.: Interrater reliability: the kappa statistic, Biochemia medica, 22, 276-282, 2012.
- 396 Mesman, J. P., Ayala, A. I., Goyette, S., Kasparian, J., Marcé, R., Markensten, H., Stelzer, J. A. A., Thayne, M. W., Thomas,  
397 M. K., Pierson, D. C., and Ibelings, B. W.: Drivers of phytoplankton responses to summer wind events in a stratified lake: A  
398 modeling study, Limnology and Oceanography, 67, 856-873, <https://doi.org/10.1002/lno.12040>, 2022.
- 399 Moras, S., Ayala, A. I., and Pierson, D. C.: Historical modelling of changes in Lake Erken thermal conditions, Hydrology  
400 and Earth System Sciences, 23, 5001-5016, 2019.
- 401 Nelson, N. G., Muñoz-Carpena, R., Philips, E. J., Kaplan, D., Sucsy, P., and Hendrickson, J.: Revealing Biotic and Abiotic  
402 Controls of Harmful Algal Blooms in a Shallow Subtropical Lake through Statistical Machine Learning, Environmental  
403 Science & Technology, 52, 3527-3535, 10.1021/acs.est.7b05884, 2018.
- 404 Paerl, H. W.: Nuisance phytoplankton blooms in coastal, estuarine, and inland waters1, Limnology and Oceanography, 33,  
405 823-843, 10.4319/lno.1988.33.4part2.0823, 1988.
- 406 Paerl, H. W. and Huisman, J.: Blooms Like It Hot, Science, 320, 57-58, doi:10.1126/science.1155398, 2008.
- 407 Persson, I. and Jones, I. D.: The effect of water colour on lake hydrodynamics: a modelling study, Freshwater Biology, 53,  
408 2345-2355, <https://doi.org/10.1111/j.1365-2427.2008.02049.x>, 2008.
- 409 Pettersson, K.: The Availability of Phosphorus and the Species Composition of the Spring Phytoplankton in Lake Erken,  
410 Internationale Revue der gesamten Hydrobiologie und Hydrographie, 70, 527-546, 10.1002/iroh.19850700407, 1985.
- 411 Pettersson, K.: Mechanisms for internal loading of phosphorus in lakes, Hydrobiologia, 373, 21-25,  
412 10.1023/A:1017011420035, 1998.
- 413 Pettersson, K., Grust, K., Weyhenmeyer, G., and Blenckner, T.: Seasonality of chlorophyll and nutrients in Lake Erken –  
414 effects of weather conditions, Hydrobiologia, 506, 75-81, 10.1023/B:HYDR.000008582.61851.76, 2003.
- 415 Pierson, D. C., Pettersson, K., and Istvanovics, V.: Temporal changes in biomass specific photosynthesis during the summer:  
416 regulation by environmental factors and the importance of phytoplankton succession, Hydrobiologia, 243, 119-135,  
417 10.1007/BF00007027, 1992.
- 418 Read, J. S., Hamilton, D. P., Jones, I. D., Muraoka, K., Winslow, L. A., Kroiss, R., Wu, C. H., and Gaiser, E.: Derivation of  
419 lake mixing and stratification indices from high-resolution lake buoy data, Environmental Modelling & Software, 26, 1325-  
420 1336, 10.1016/j.envsoft.2011.05.006, 2011.
- 421 Recknagel, F., Fukushima, T., Hanazato, T., Takamura, N., and Wilson, H.: Modelling and prediction of phyto- and  
422 zooplankton dynamics in Lake Kasumigaura by artificial neural networks, Lakes & Reservoirs: Science, Policy and  
423 Management for Sustainable Use, 3, 123-133, 10.1111/j.1440-1770.1998.tb00039.x, 1998.
- 424 Reichwaldt, E. S. and Ghadouani, A.: Effects of rainfall patterns on toxic cyanobacterial blooms in a changing climate:  
425 Between simplistic scenarios and complex dynamics, Water Research, 46, 1372-1393, 10.1016/j.watres.2011.11.052, 2012.
- 426 Richardson, J., Miller, C., Maberly, S. C., Taylor, P., Globevnik, L., Hunter, P., Jeppesen, E., Mischke, U., Moe, S. J.,  
427 Pasztaleniec, A., Søndergaard, M., and Carvalho, L.: Effects of multiple stressors on cyanobacteria abundance vary with lake  
428 type, Global Change Biology, 24, 5044-5055, 10.1111/gcb.14396, 2018.
- 429 Rousso, B. Z., Bertone, E., Stewart, R., and Hamilton, D. P.: A systematic literature review of forecasting and predictive  
430 models for cyanobacteria blooms in freshwater lakes, Water Research, 182, 115959, 10.1016/j.watres.2020.115959, 2020.
- 431 Stanley, F. K. T., Irvine, J. L., Jacques, W. R., Salgia, S. R., Innes, D. G., Winquist, B. D., Torr, D., Brenner, D. R., and  
432 Goodarzi, A. A.: Radon exposure is rising steadily within the modern North American residential environment, and is  
433 increasingly uniform across seasons, Scientific Reports, 9, 18472, 10.1038/s41598-019-54891-8, 2019.
- 434 Watson, S. B., Miller, C., Arhonditsis, G., Boyer, G. L., Carmichael, W., Charlton, M. N., Confesor, R., Depew, D. C.,  
435 Höök, T. O., Ludsın, S. A., Matisoff, G., McElmurry, S. P., Murray, M. W., Peter Richards, R., Rao, Y. R., Steffen, M. M.,  
436 and Wilhelm, S. W.: The re-eutrophication of Lake Erie: Harmful algal blooms and hypoxia, Harmful Algae, 56, 44-66,  
437 <https://doi.org/10.1016/j.hal.2016.04.010>, 2016.
- 438 Wei, B., Sugiura, N., and Maekawa, T.: Use of artificial neural network in the prediction of algal blooms, Water Research,  
439 35, 2022-2028, 10.1016/S0043-1354(00)00464-4, 2001.
- 440 Xiao, X., He, J., Huang, H., Miller, T. R., Christakos, G., Reichwaldt, E. S., Ghadouani, A., Lin, S., Xu, X., and Shi, J.: A  
441 novel single-parameter approach for forecasting algal blooms, Water Research, 108, 222-231, 10.1016/j.watres.2016.10.076,  
442 2017.



443 Yang, Y., Stenger-Kovács, C., Padisák, J., and Pettersson, K.: Effects of winter severity on spring phytoplankton  
444 development in a temperate lake (Lake Erken, Sweden), *Hydrobiologia*, 780, 47-57, 10.1007/s10750-016-2777-8, 2016.  
445  
446